CHAPTER III
RESULTS

3. 1 FTIR

Assignment of the peaks of the IR spectrum of polyimide conformation had been reported by Ishida et.al. (1980). The most widely used band for monitoring of imide formation are imide absorptions near 1778 cm^{-1} (symmetrical stretch, C=O), 1380 cm^{-1} (C-N stretch) and 725 cm^{-1} (bending of C=O). As seen in Figures 6 (a)-(c), all of the imide absorption bands were observed in each polyimide film as shown in Table 1

Table 1 Bands assignments of the peaks changs when varying the final curing temperature of BPDA-PDA, PMDA-ODA and BTDA-ODA/MPD polyimide films

Frequency (cm^{-1})	Vibrational mode
1778	symmetric stretch of carbonyl group (C=O) of imide absorption
1720	asymmetric stretch n(C=O)
1670	amide carbonyl stretching
1600	aromatic ring stretch ν_{16} 1,4 C_6H_4
1500	aromatic ring stretch ν_{13} 1,4 C_6H_5
1410	symmetric stretch of the carboxylate ion (COO^-)
1380	C-N stretch of imide absorption
1240	ether C-O-C and anhydride C-O-C asymmetric stretch
1015	aromatic vibration ν_6 1,2,4,5-C_6H_2
725	carbonyl (C=O) bending

Figures 6 (a)-(c) show the effect of final curing temperature on the FTIR spectra of the BPDA-PDA, PMDA-ODA and BTDA-ODA/MPD. At the final curing temperature of 100°C, the imide was formed initially as observed from the bands near 1778 cm^{-1}. But the imide absorption bands at 1380 cm^{-1} and 725 cm^{-1} were hardly seen at 100°C. The strong band near 1670 cm^{-1} of amide carbonyl stretch, the symmetrical stretch of the carboxylate ion (COO^-) near 1410 cm^{-1} and the ether and anhydride C-O-C stretch at 1240 cm^{-1} were observed in the spectra indicated that the poly(amic acid)s precursors remained in the polyimide cured at 100-150°C. Above 150°C the bands representing the vibration of the poly(amic acid)s had disappeared and the bands of the imide absorption occurred instead. The absorption bands of the imide group increased in intensities with the increase in the final curing temperature. The degree of imidization was monitored from the change in peak height near 1778 cm^{-1}. This was normalized against an internal aromatic absorption band due to the independence of peak height or intensity on the curing temperature.

The relative degree of imidization was calculated from equation (2). The samples were imidized initially less than 20% at the final curing temperature of 100°C. At 200°C the flexible chain BTDA-ODA/MPD was almost completely imidized whereas the semirigid BPDA/PDA and semiflexible PMDA-ODA were nearly fully imidized at 250°C. The zero error bars at 400°C for BPDA-PDA, 350°C in PMDA-ODA and BTDA-ODA/MPD were due to the highest peak height ratio at 1780 to 1015 cm^{-1}. This shows that the flexible chain BTDA-ODA/MPD PAA has experienced the ring closure to form the resulting polyimide at lower curing temperature than the semirigid and semiflexible PAA.

Pryde (1989) found that the bands near 1778 and 720 cm^{-1} are affected by anhydride absorption that appear during the thermal cycle. This interference can result in significant error in determining the degree of imidization, particularly when the 1778 cm^{-1} band is used. The imide band near 1380 cm^{-1}, however, does not appear to be affected by any other absorbance. In Figure 8, percent conversion of polyimide films plotted as a function of curing temperature is shown. The degree of imidization increases with the increase in the curing temperature; the same trend can be observed in the graph of the degree of imidization with respect to the peak height monitoring near 1778 cm^{-1} in Figure 7.

(a) PI-2610 (BPDA-PPD)

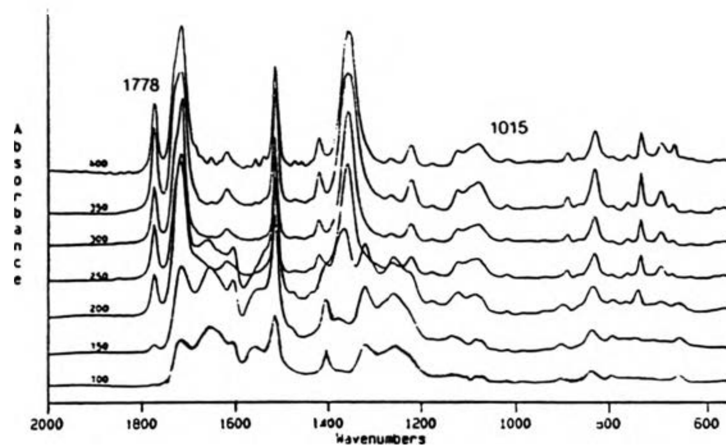

(b)PI-2540 (PMDA-ODA)

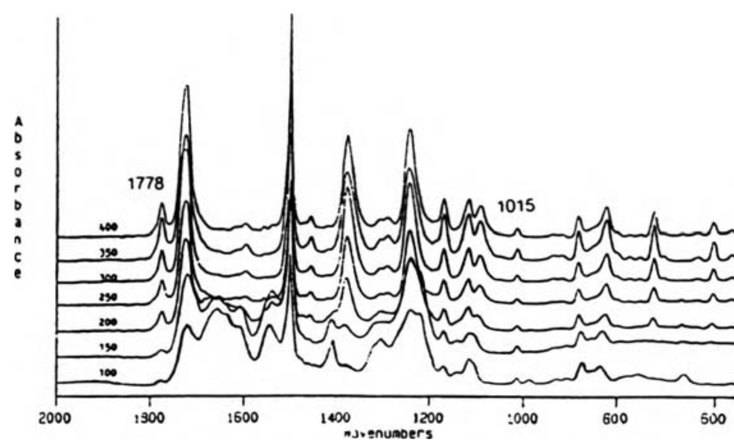

(c)PI-2579 (BTDA-ODA/MPD)

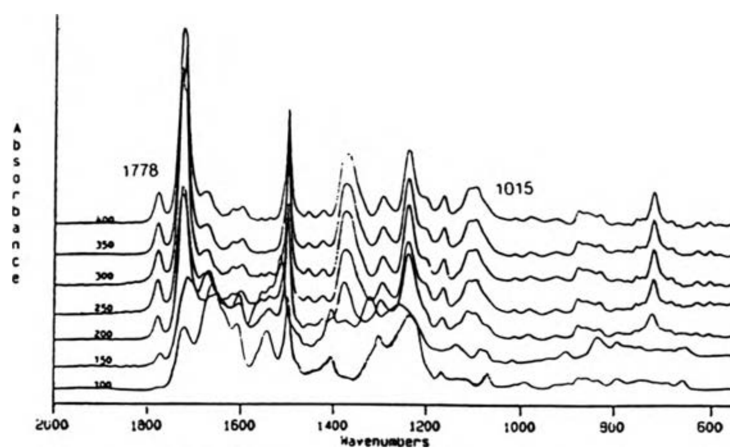

Figure 6 Effect of curing temperature on the FTIR spectra of (a) BPDA-PDA (PI-2610) (b) PMDA-ODA (PI-2540) and (c) BTDA-ODA/MPD (PI-2579).

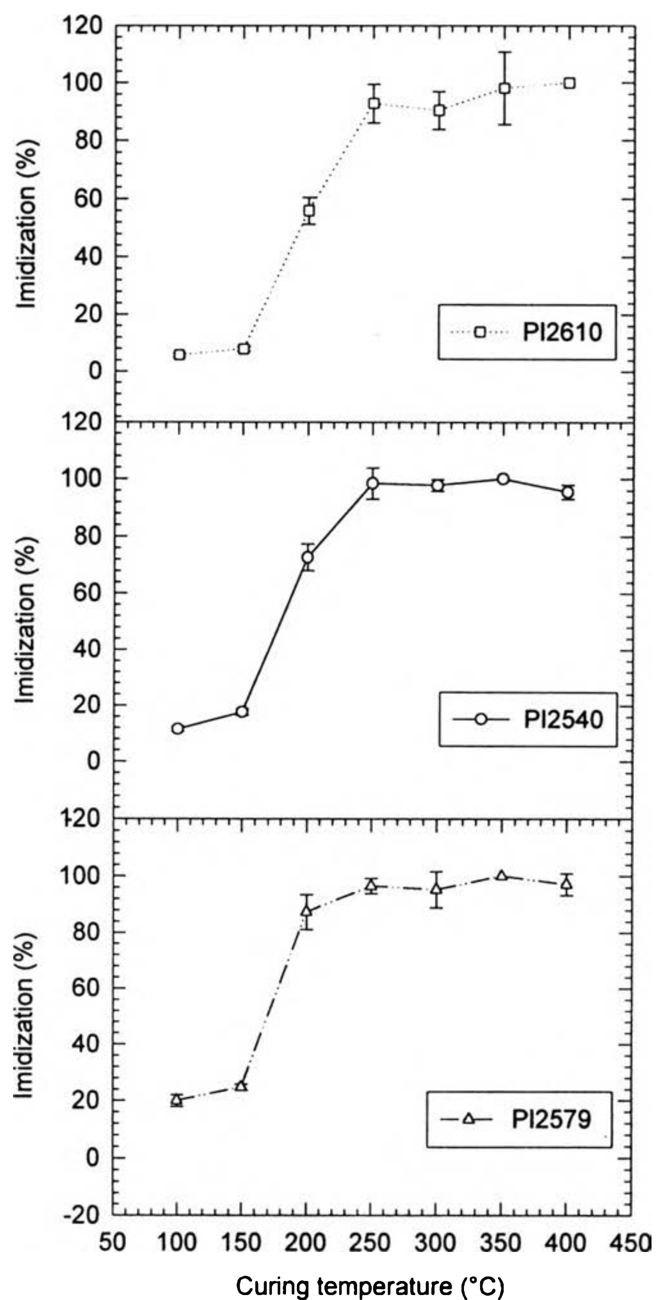

Figure 7 Percent conversion of imidization plotted as a function of curing temperature for the films from the peak height ratio calculated at the frequency of 1778 cm-1 and normalized with 1015 cm^{-1}.

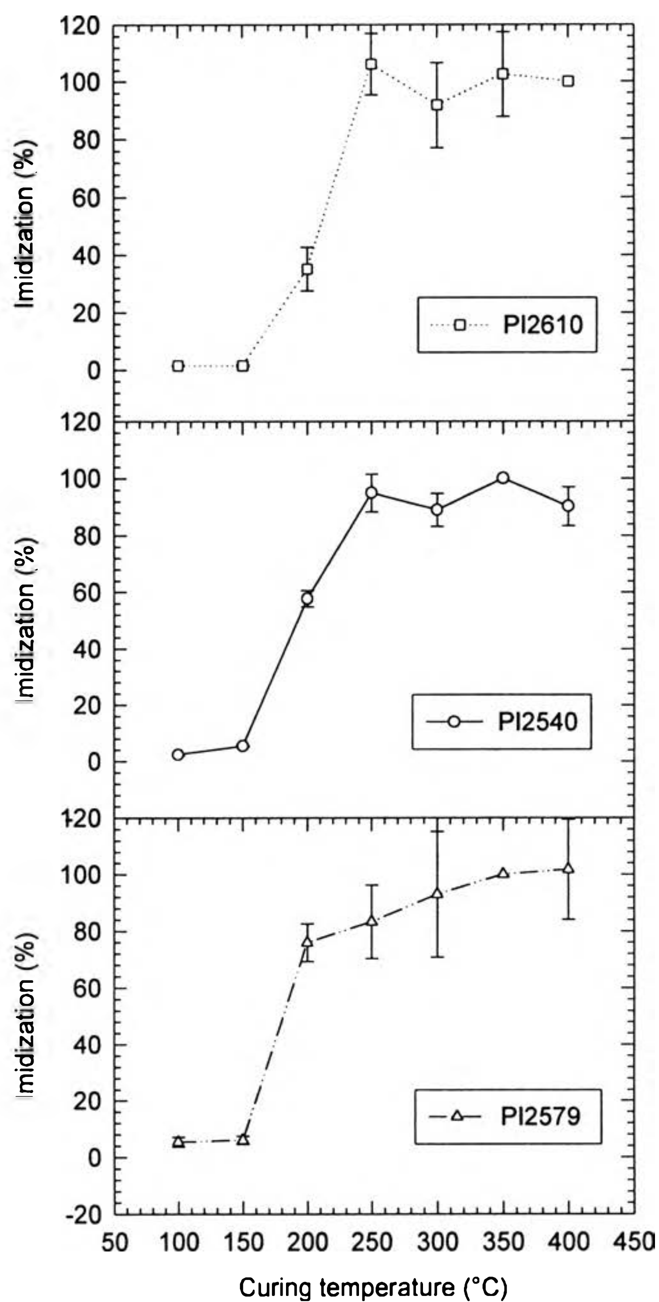

Figure 8 Percent conversion of imidization plotted as a function of curing temperature for the films from the peak height ratio calculated at the frequency of 1380 cm^{-1} and normalized with 1015 cm^{-1}.

The next interesting parameter on the degree of imidization was the effect of curing rate. Figure 7 shows the peak height ratio of the bands at 1780 cm^{-1} and 1015 cm^{-1} plotted as a function of curing rate. It is shown here that the curing rate does not affect the degree of imidization at the curing rates ranging from 1 to 8°C/minute. The higher the peak height ratio is, the greater the percent conversion of the polyimide film is. Obviously, the semirigid BPDA-PDA films shows the highest degree of imidization, followed by the flexible chain, BTDA-PDA/MPD films. The semiflexible chain, PMDA-PDA has the lowest degree of imidization. The possible reason for this result is that the intermolecular links reactions may occur during thermal curing which would interfere the ring closure of the flexible chain rather than that of the semirigid chain structure as reported by Snyder et.al. (1989).

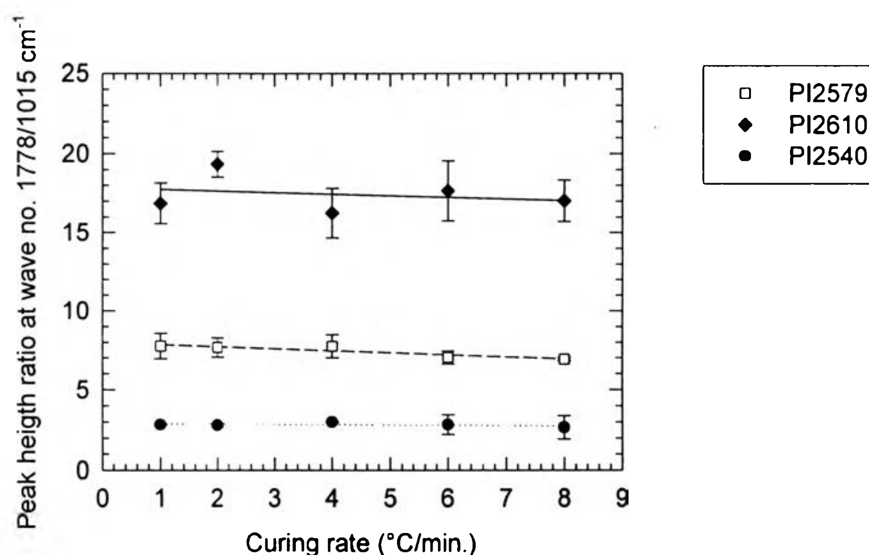

Figure 9 The effect of curing rate on the degree of imidization of the polyimide films cured at 400°C for 30 minutes.

3.2 WAXD

The wide angle reflection X-ray spectra of BPDA-PPD (PI-2610), PMDA-ODA (PI-2540) and BTDA-ODA/MPD (PI-2579) polyimide films cured at 400°C for 30 minutes are shown in Figures 10 (a)-(c). All of the films show the broad band at the $2\theta \approx 22°$ indicating that the film does not prefer orientation when coated on the glass substrate and a poor intermolecular packing of the films

Figures 11(a)-(c) show the diffraction X-ray bands of the polyimide films on the silicon wafer. The sharp peak at 37° is the reflection peak due to the crystal of silicon. The broad band at around 22° in Figure 11(a) of the BPDA-PPD (PI-2610) films is due to the diffraction from the semicrystalline of polyimide films on the substrate. For the PMDA-ODA (PI-2540) and BTDA-ODA/MPD (PI-2579) films, even the broad bands were not observed, suggesting a highly amorphous nature of the films. It appears that the presense of the silicon substrate enhances the unorientation character of the polyimide films.

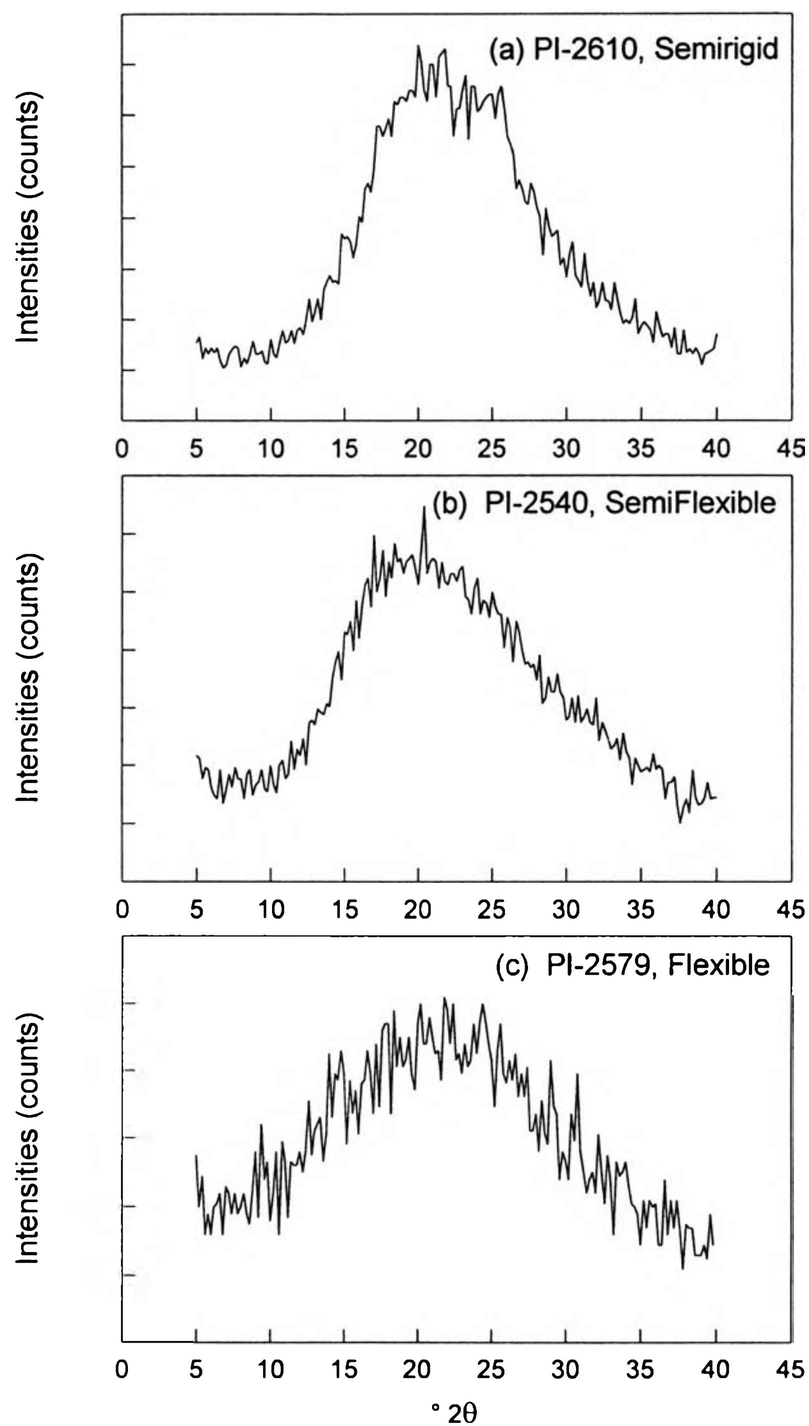

Figure 10 The Wide angle X-ray spectra of the polyimide films on the glass substrate (a) BPDA-PPD, (b) PMDA-ODA and (c) BTDA-ODA/MPD.

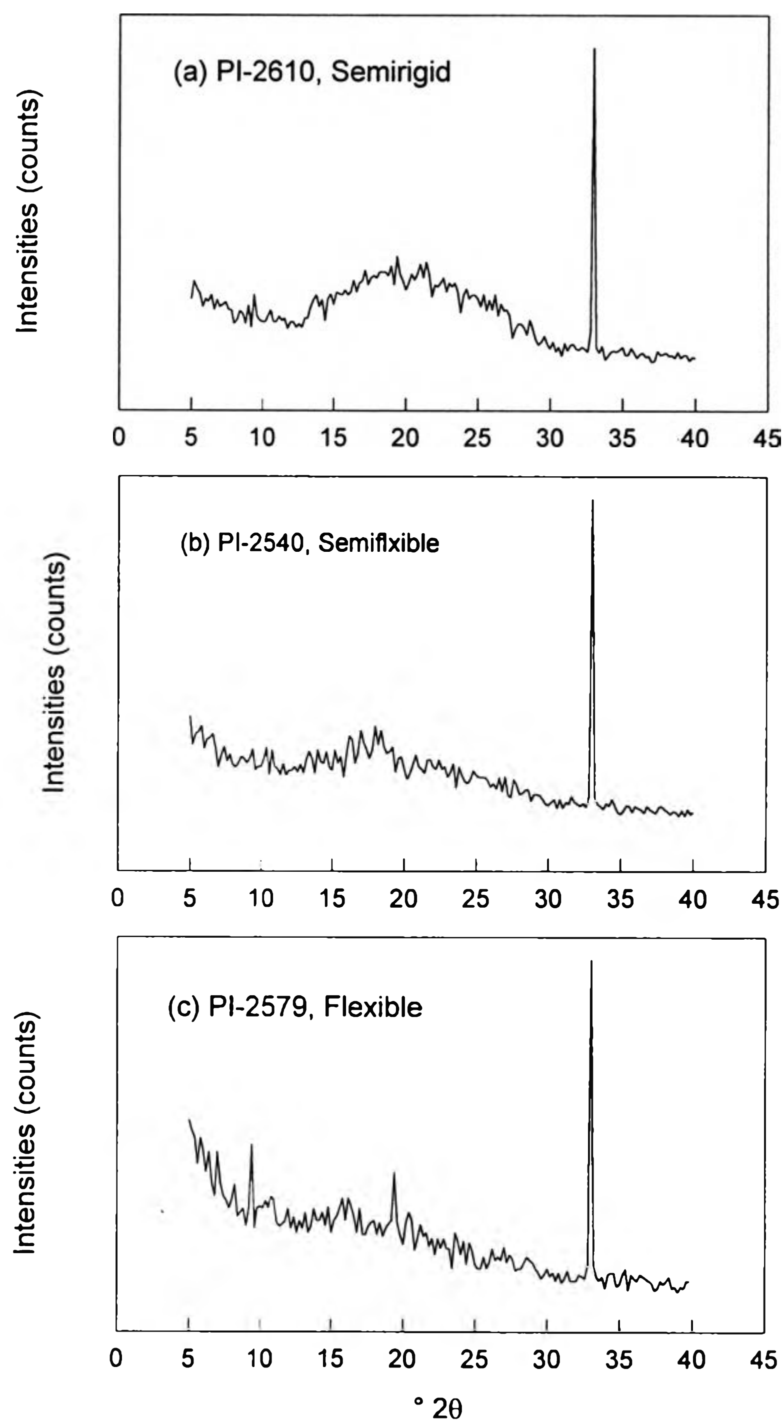

Figure 11 **The Wide angle X-ray spectra of the polyimide films on silicon wafer (a) BPDA-PPD, (b) PMDA-ODA and (c) BTDA-ODA/MPD.**

3.3 TGA

The thermal stability of the polyimide films was evaluated by thermogravimetric analysis. Figure 12 shows the thermogram of the films cured at a high curing temperature and a low curing temperature. At the low curing temperature (100-200°C), a particular thermogram was divided into four different regimes. The first and second regimens cannot be seen in the higher curing temperature film (250-400°C). Before discussing the thermal stability of the polyimide films, the definition of each regime will be described.

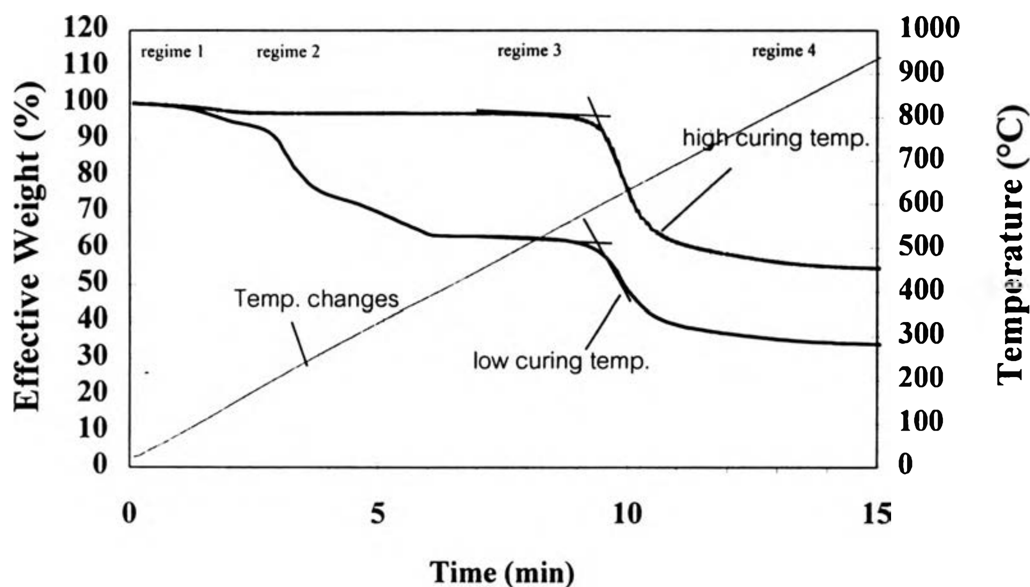

Figure 12 Thermogram of the films cured at low and high temperature for 30 minutes shows the four different regimes.

1st regime: The first transition of the weight with the temperature. The onset transition temperature is corresponding to 100°C which is the boiling point of water.

2nd regime: The weight change in this regime is due to the evaporation of N-methyl-2-pyrolidone (NMP) which is the solvent in the poly(amic acid) solution. The boiling temperature of NMP is ~ 202°C.

3rd regime: The rapid decrease in weight of the polyimide chain indicates a degradation. Degradation temperature is defined as the temperature at which the polyimide films are decomposed. This parameter can be used to determine the thermal stability of the film.

4th regime: All of the polyimide chains are degraded and only organic hydrocarbons remain. The weight decreases asymptotically. The remaining weight of the samples can also be used for determining the thermal stability.

A slight reduction of the weight in regime 1 was observed at all curing temperatures because of the moisture absorbed by the films when kept in room air. When the final curing temperature was below 250°C, some of the poly(amic acid)s was left in the samples. Some water from the by-product of the thermal curing process and from the environment was trapped in the samples. Regime 1 was more noticeable in films cured at low temperature than in films cured above 250°C which contained only the water from the environment.

The transition in the second regime was attributed to the evaporation of NMP and decomplexation of poly(amic acid)s and NMP. During evaporation, poly(amic acid)s films dried to the solid state still contain some amount of solvent. This is due to the formation of stable complexes of poly(amic acid) and solvent in dried films as reported by Brekner and Feger, (1987). The

complex formation is shown in Figure 13 involving hydrogen bonds which take an active part. The characteristic temperatures for the second regime of TGA curves are shown in Figure 14. Thermal stability of the complexes was determined from the characteristic temperatures. These temperatures, however, were observed at the curing temperature below 250°C because some of the solvent was trapped and diffused into the film which was crossed-link and imidized to the polyimide. Thermal stability is an important factor for the application of polyimide films in microelectronic gas sensors, where the silicon array must be exposed to sudden high temperature increases.

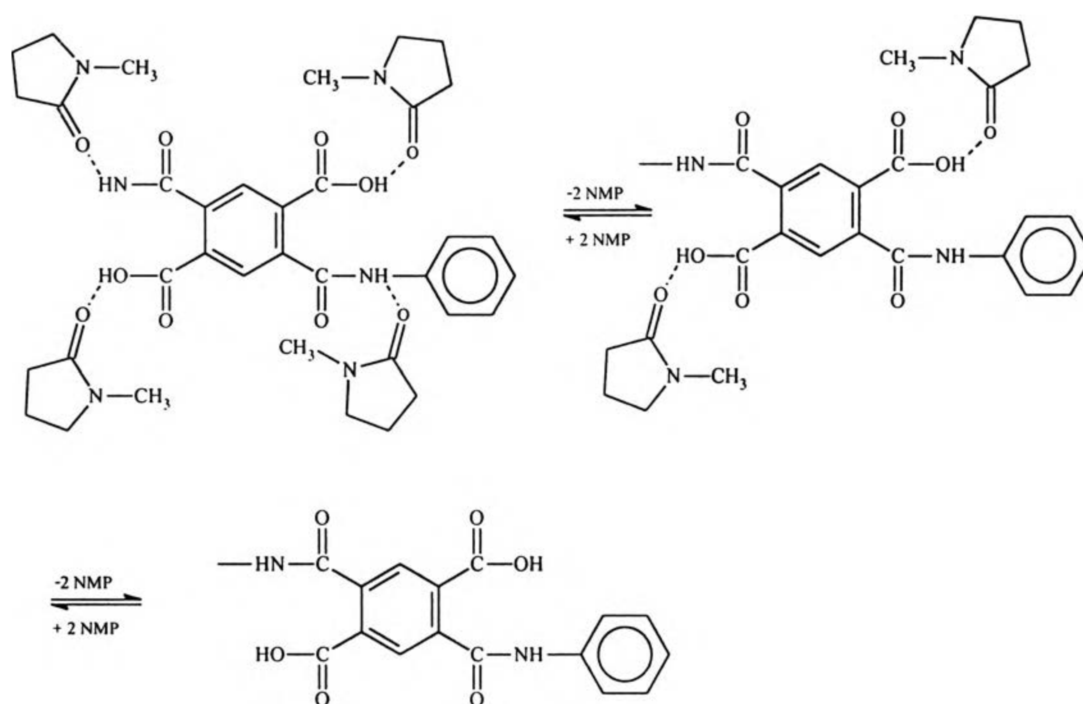

Figure 13 Hydrogen bonding in the complexes of the ploy(amic acid and the NMP solvent.

A study of the thermal stability of the films by thermogravimetric analysis at the low scanning rate (10 K/minute) and high scanning rate (60° K/minute) are shown in Figures 15 (a)-(b). The decomplexation temperature of

the film scanned at high rate is higher than at the lower rate. This can be attributed to the thermal lag in the high scanning rate.

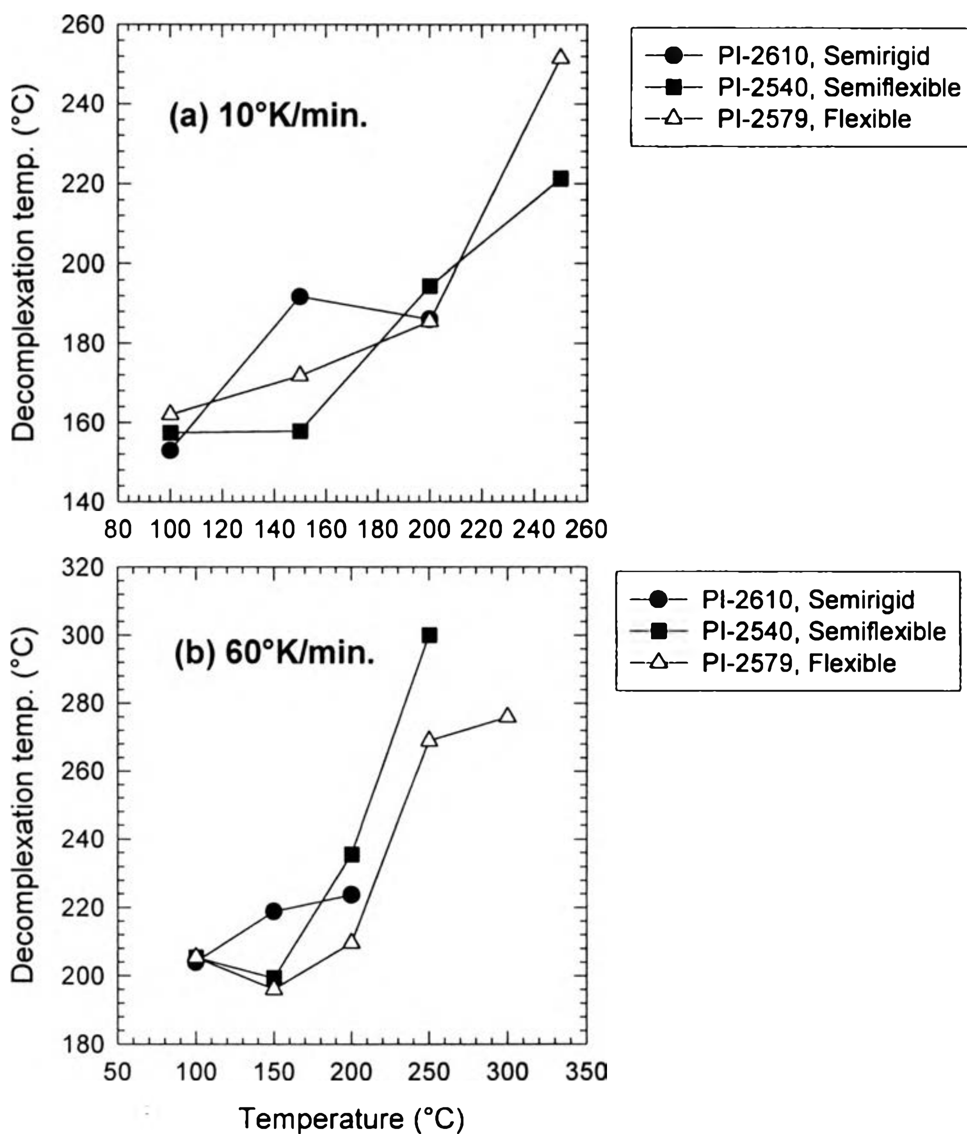

Figure 14 The decomplexation temperature of different curing films at scanning rate of (a) 10°K/min. and (b) 60°K/min.

I 17684377

In the third regime, after the decomplexation of poly(amic acid) occurred, the cyclodehydration involves only amic acid groups which were free from solvent. The decomposition of complexes, imidization, and some cross-linking reactions were accompanied by evolution of volatile products. Weight loss after the second regime is constant due to the imidization, and because some cross-linking occurred. Weight losses above 250°C were related to the decomposition of only polyimide as seen in FTIR results. The degradation temperature involved in this regime can be investigated to determine thermal stability. Weight losses in the third regime were also compared between the three polyimdes at different scanning rates. The weight loss at low scanning rate and high scanning rate cannot be distinquished. The degradation temperature (T_d) shows the same trend as the decomplexation temperature in the second regime. Regarding thermal stability, we found that the polyimides are stable up to 618°C (BPDA-PPD). At higher temperature, degradation started to set in accompanied by significant weight loss. The effect of broad ranges of curing rate on the decomposition of the complexes PAA vs NMP was studied by Brekner and coworkers, (1987). In addition, Corburn and Pottiger (1994) evaluated the effect of curing rate on the structure, properties and stress development in PMDA-ODA and BPDA-PPD films. They varied the curing rate from 1°C/minute to 100°C/minute. In this experiment, a shorter range of curing rate on the thermal stability of polyimide from 1°C/minute to 8°C/minute was studied as follows:

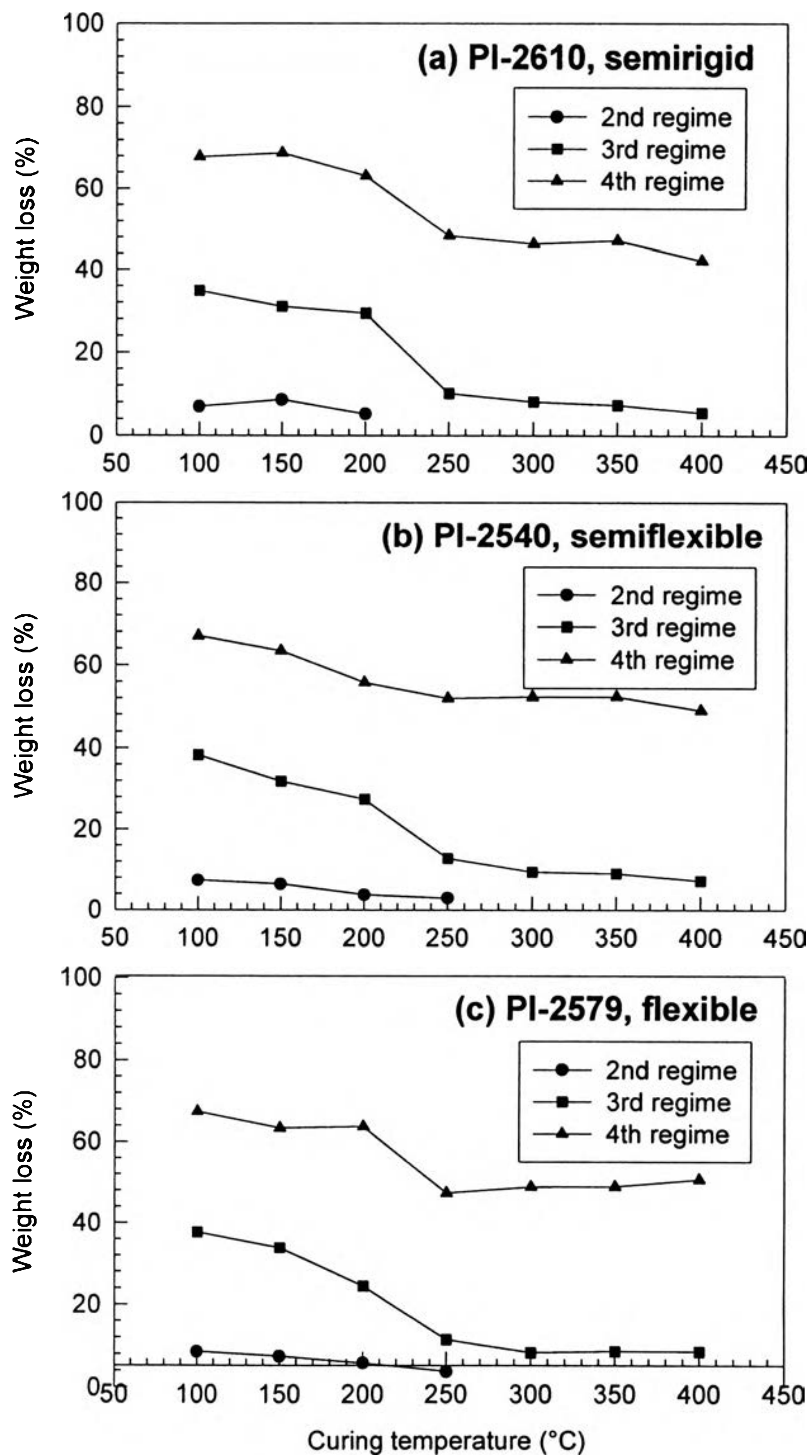

Figure 15 Weight loss of polyimide films at various curing temperatures scanned at the rate of 10°K/min.

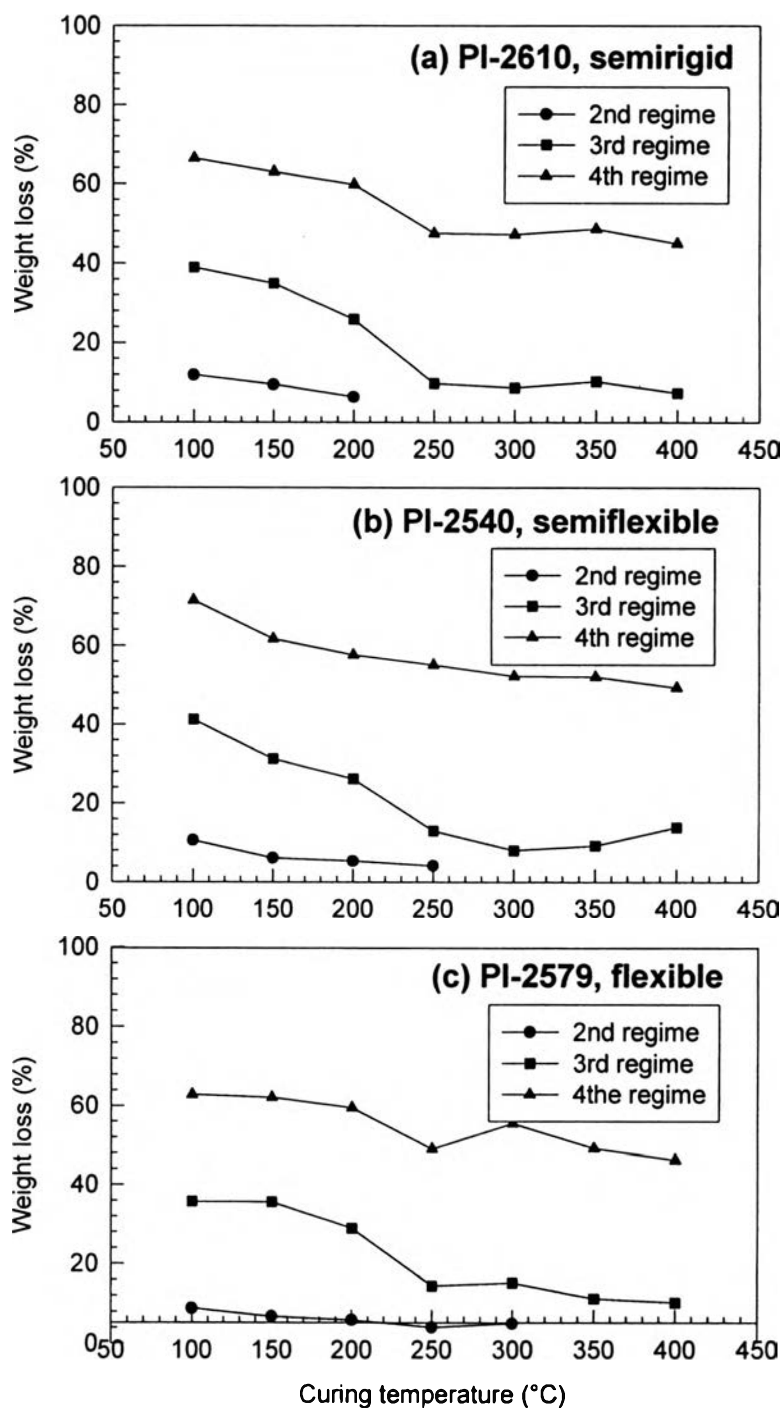

Figure 16 Weight loss of polyimide films at various curing temperatures scanned at the rate of 60°K/min.

3.2.1 Effect of Curing Temperature

There was some degree of imidization above 100°C for curing temperature (Figure 7). So, the degradation temperature of the polyimide can still be observed even at low curing temperatures. We can see that T_d is independent of the curing temperature (Figure 17). But it can depend on the chemical structures of the polyimides. The most rigid chain structure, BPDA-PPD, is the most stable up to 618°C for the 60°K/minute scanning rate of the thermogram, followed by the PMDA-ODA, the semiflexible chain. The flexible chain gives the lowest degradation temperature.

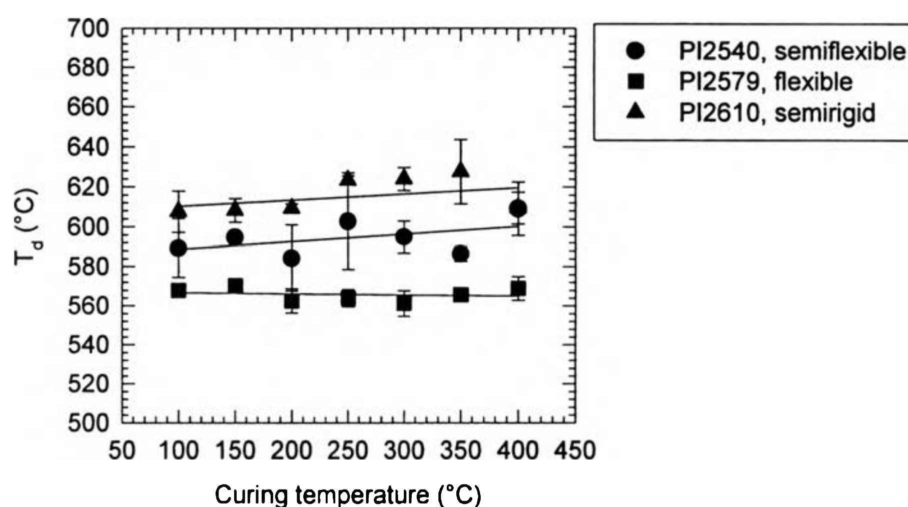

Figure 17 No correlation of the degradation temperature of polyimide films with the curing temperature.

3.2.2 Effect of Curing Rate

The former work of Pottiger and Corburn (1994) showed that the degradation temperature in films formed at more rapid curing rate was higher than that of the films cured at lower rate. In our experiment, a narrower range of curing rates was studied. Our result shows that the T_d is independent of the

curing rate and is consistent with the result of Pottiger and Corburn (1994) for the effect of curing temperature, as shown in Figure 18.

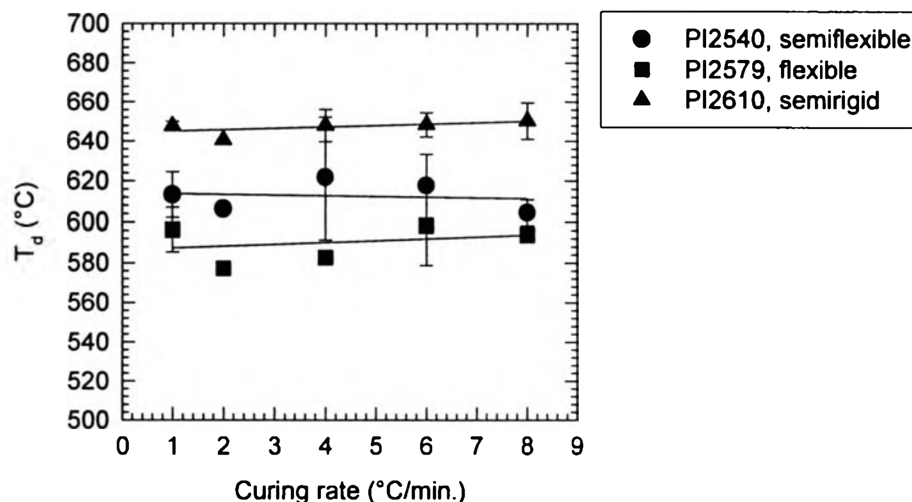

Figure 18 No correlation of thermal degradation of polyimide films with the curing rate.

3.2.3 Effect of Curing Time

It is expected that, the thermal stability should be affected by the curing time. We varied the curing time of the polyimide films of the most stable film BPDA-PPD. The degradation temperature (T_d), however, does not change with increasing curing time from 30 minutes to 240 minutes (Figure 19). For the thermal stability determination, the chemical structure is the most important parameter that controls the stability of the films.

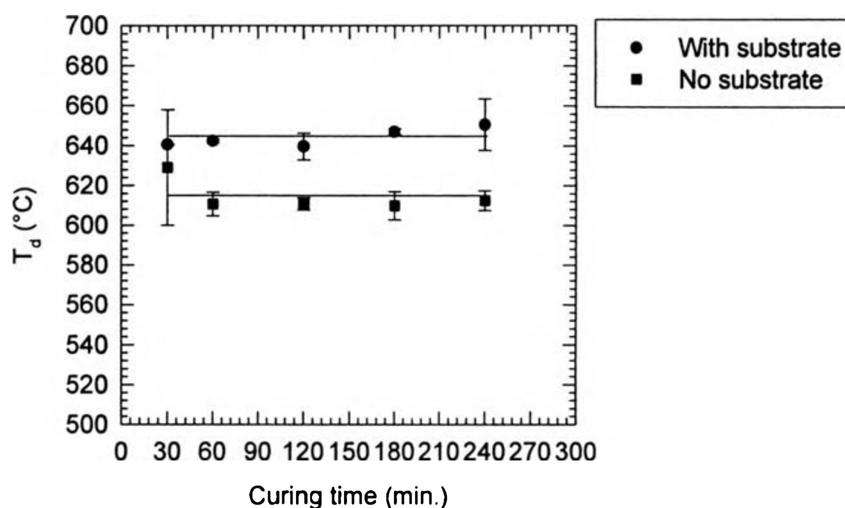

Figure 19 No correlation of curing time and the degradation temperature of PI-2610 films with substrate and without substrate.

3.2.4 Effect of Substrate

We tried to mimic the real situation during vapor deposition of platinum onto the silicon wafer which has to be exposed to a high temperature. So, the polyimide films on the silicon wafer were studied. In Figure 19, T_d of the film on the silicon wafer was 30°C higher than the bare BPDA-PPD film. A possible reason for this result is the thermal inertia of the heat transfer mode. In addition, the other reason is instrumental artifact effect on the film on the substrate. The electrical noise error in the weight monitoring of the film on the substrate might be another reason for the difference in T_d of the film on the substrate and the bare film. As seen in the thermogram in Figure 18, the weight loss in the fourth regime of the BPDA-PPD film on the silicon wafer is lower than that of the bare film for 20%. At the moment, we do not know the exact reason for this behavior.

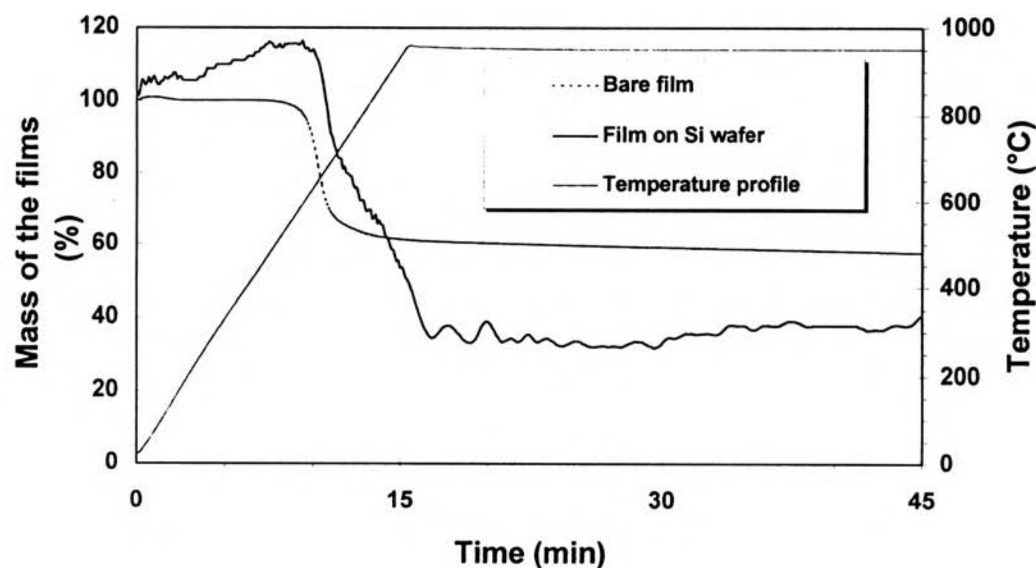

Figure 20 Effect of substrate on T_d of PI-2610 films cured at 400°C for 30 minutes.

A summary of the degradation temperatures of the three different polyimides is shown in Table 2 below:

Table 2 Summaries table of T_d of polyimide films

Polyimide films	Bare film at heating rate		Film on Si wafer
	10°K/minute	60°K/minute	
BPDA-PPD (PI-2610), semirigid	584 ± 22 °C	588 ± 22 °C	615 ± 22 °C
PMDA-ODA(PI-2540), semiflexible	610 ± 22 °C	616 ± 13 °C	646 ± 7 °C
BTDA-ODA/MPD (PI-2579), flexible	566 ± 5 °C	567 ± 5 °C	598 ± 16 °C

3.4 TMA

The coefficient of linear thermal expansion (CTE) of polyimide films was measured using a thermomechanical analysis. In the case of thin polymer films, this technique is usually limited to measure in-plane CTE (α_{xy}) using the extension probe rather than the out-of-plane CTE (α_z), because of the sensitivity of the instrument is limited to 1×10^{-6} /°C. However, the comparison of the α_{xy} and α_z was investigated using TMA. There was a systematic error from the α_z measurement, but we wanted to compare to α_z in each polyimde film, so only qualitative comparisons will be assessed.

3.4.1 In-plane CTE (α_{xy}) of Polyimide Films

The average CTE was defined by equation (1). Typical plots of the variation of the CTE with temperature of the semirigid, semiflexible and flexible films are given in Figure 21. The average in-plane CTE of polyimide films were determined by averaging CTE values over the temperature range of 50 to 300 °C. The nominal film thickness was about 25 μm. The results are 18 ± 0.3 ($\times10^{-6}$ °C^{-1}) for the semirigid, 43 ± 2 ($\times10^{-6}$ °C^{-1}) for the semiflexible PMDA-ODA, and 54 ± 4 ($\times10^{-6}$ °C^{-1}) for the flexible BTDA-ODA/MPD. These data showed that the more rigid the chain structure, the lower the in-plane CTE value was.

The expansion temperature (T_e) is the temperature at which the fully imidized film starts to stretch and is defined as the temperature where CTE starts to vary nonlinearly with temperature. Nomally it is above T_g. The expansion temperature can be used to characterize the expansion behavior of the film. Similarly, we can define the yielding temperature to be the temperature at which the film elongation deviates from linearity as determined by a 0.2 % elongation offset. The yielding temperature can compliment the

expansion temperature on providing us with the thermal expansion behavior of thin films investigated. Even though the procedures to determine these two parameters are different, they give nearly the same information with respect to the expansion behavior of different polyimide chain structures. The data of the expansion temperature (T_e) and the yielding temperature (T_y) are summarized in Table 2. We can see that the more rigid the polyimide film is, the lower the expansion temperature and yielding temperature become. Surprisingly, we find that the expansion temperature of the semiflexible film, PMDA-ODA has a higher value than that of the semirigid one which requires more thermal energy to change the chain conformation. Looking at the stability of the chemical structure of PMDA-ODA, we notice that it has a more stable structure due to the fact that the lone pair on the oxygen in the ether linkage can delocalize along the polymer chain. But the electron in the semirigid BPDA-PPD polyimide film cannot delocalize the whole chain, owing to the non-conjugate nature at the C-C linkage of the two phenyl rings in the dianhydride segment. Therefore, the more stable structure of the semiflexible PMDA-ODA needs more thermal energy to accompany the chain conformation or movement. Normally, a flexible chain structure moves easier than a rigid chain structure, so T_e and T_y of the more flexible chain (BTDA-ODA/MPD) are higher than that of the less flexible one.

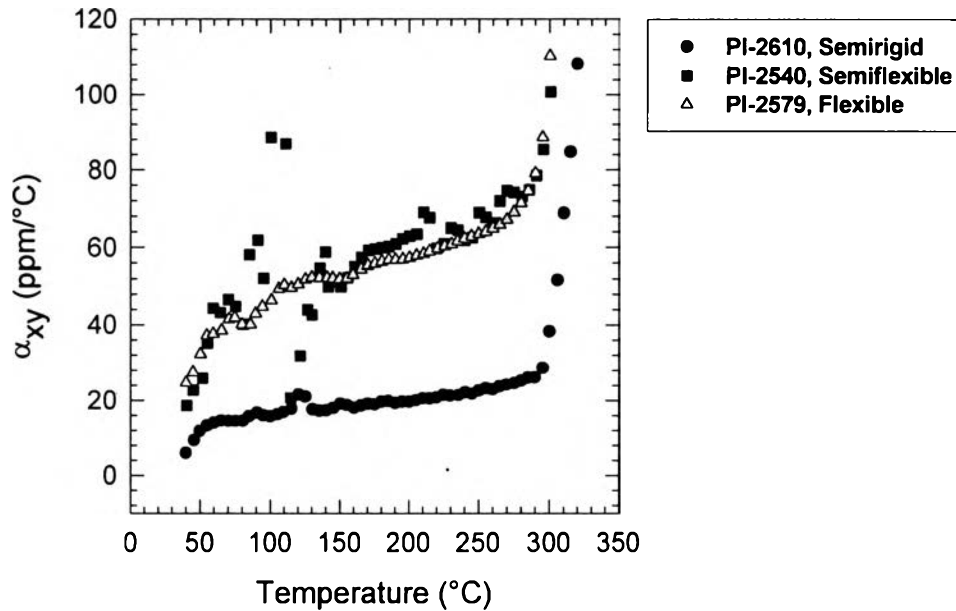

Figure 21 The plots of the in-plane CTE versus temperature of polyimide.

Table 3 In-plane CTE data , expansion temperature and yielding temprature of polyimide films

Polyimide	**α_{xy} ($\times10^{-6}$/°C) (50-300°C)**	**T_e (°C)**	**T_y (°C)**
PI-2610, semirigid	18 ± 0.3	334 ± 23	352 ± 21
PI-2540, semiflexible	43 ± 2	371 ± 6	382 ± 8
PI-2579, flexible	54 ± 3	310 ± 7	318 ± 9

3.4.2 Out-of-plane CTE

In contrast, the out-of-plane CTE (α_z) of the semirigid BPDA-PPD has the highest value, followed by the semiflexible PMDA-ODA, and the flexible BTDA-ODA/MPD has the lowest out-of-plane CTE. The data of the out-of-plane CTE are summarized in Table 4.

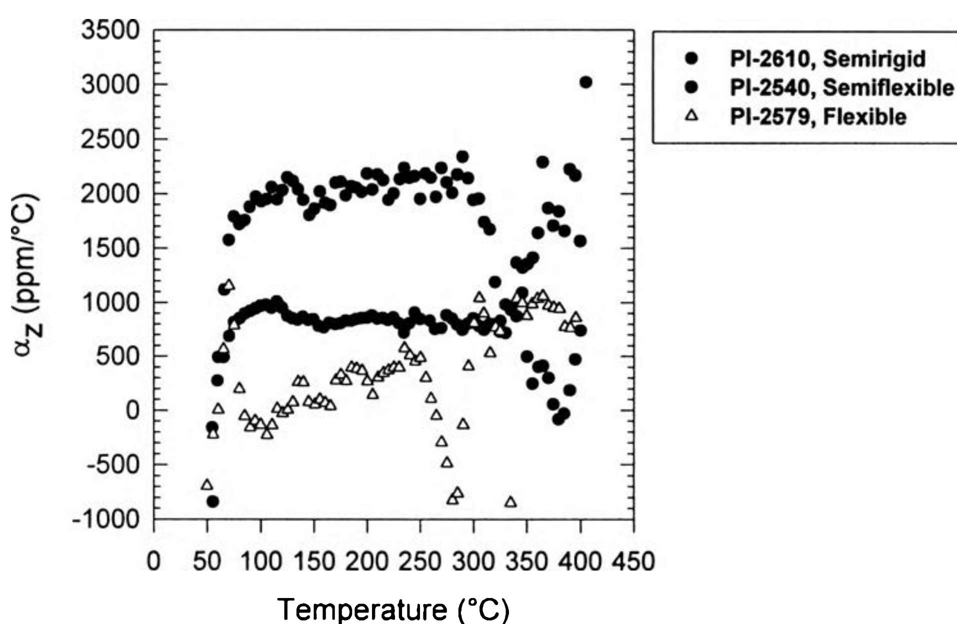

Figure 22 The out-of-plane CTE of the polyimide films.

Table 4 Out-of-plane CTE of the polyimide films

Polyimide films	CTE, α_z (ppm/°C)
PI-2610, semirigid	1881 ± 84
PI-2540, semiflexible	699 ± 99
PI-2579, flexible	215 ± 106

3.4.3 Effect of Curing Time on In-plane CTE

Figure 23 shows the average in-plane CTE of the roughly 25 μm thick polyimide films. We varied the curing time from 30 to 240 minutes. We can see that average in-plane CTE of the semirigid (BPDA-PPD) and the semiflexible (PMDA-ODA) are independent of the curing time whereas the average in-plane CTE of the flexible (BTDA-ODA/MPD) decreases slightly with curing time. The reduction in the in-plane CTE of the flexible chain may have resulted from crosslinking occuring in the long term curing as well as the flexibility of the chain. The possibility of crosslinking is more likely for the more rigid chains.

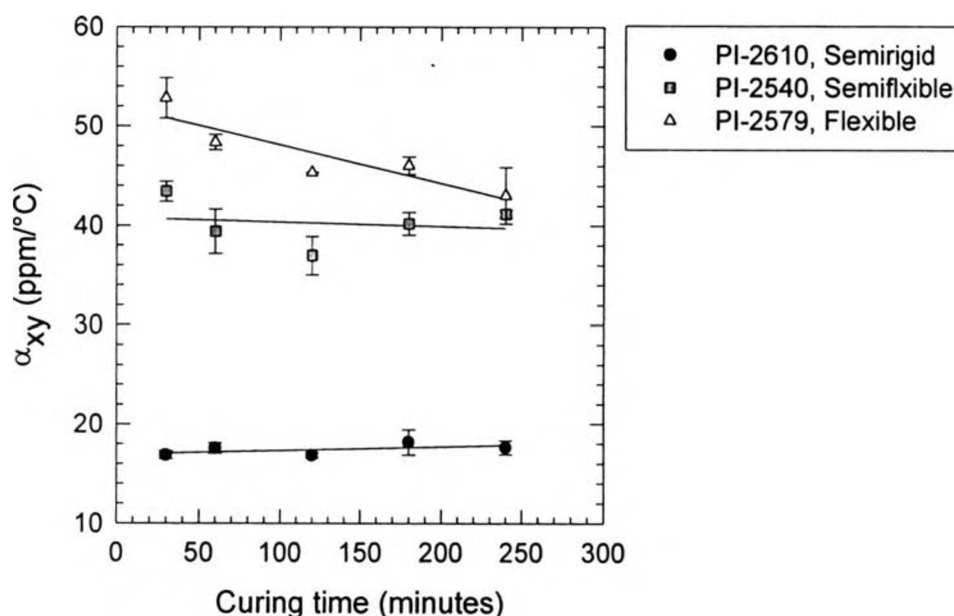

Figure 23 Effect of curing time on the mechanical properties of polyimide films.

3.4.4 Effect of Thermal Cycling on In-plane CTE of Polyimide Films

For ten cycles of thermal treatment of the polyimide films, the in-plane CTE of each film was measured and shown in Figure 24. For each cycle, we exposed the films to 300°C which is less than their glass transition temperatures (T_g) at a rate of 5 °C/minute and cooled them at the same rate to the room temperature. The in-plane CTE of the semirigid (BPDA-PDA) and semiflexible (PMDA-ODA) films hardly change after heating up and cooling down for 10 cycles. But for the flexible chain (BTDA-ODA/MPD), the in-plane CTE slightly increases. Because of its lowest expansion temperature (T_e) and yielding temperature (T_y), some parts of flexible chains might have been broken. At the each successive thermal treatment, the expansion coefficient is greater than that of the former cycle.

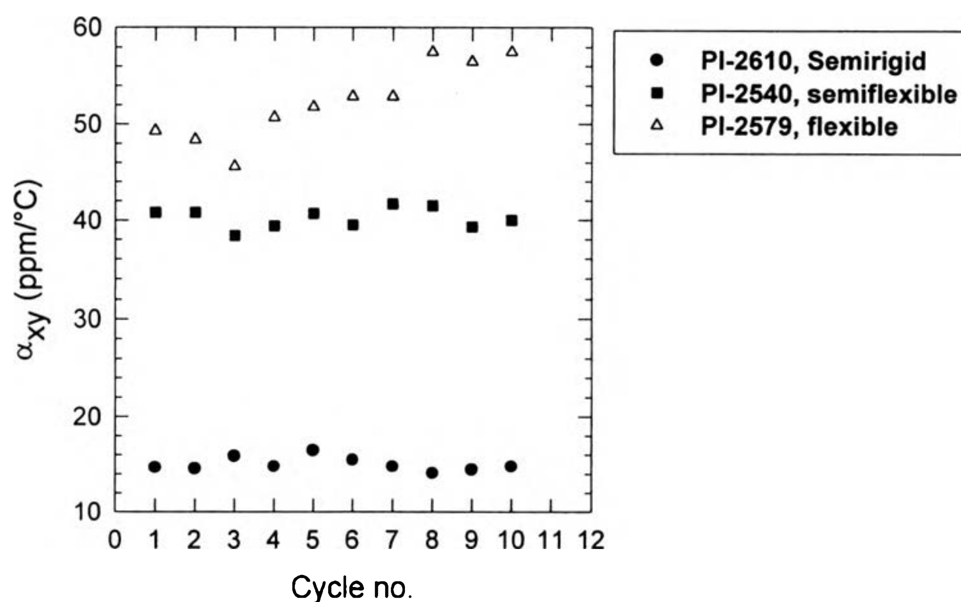

Figure 24 In-plane CTE of polyimide films at ten cycles.

3.5 Surface Topology of Polyimide on Silicon Wafer

The surface profile of polyimide was taken by optical microscopy. The viscosity of the PAA solution had significant effect on the smoothness of the films. Especially, in a small surface area of the gas sensor array, the low viscosity solution would be more advantageous than the higher viscostiy solution. As seen in the percent solid in Figure 3, the viscosity of the PI-2579 was the lowest. For the fabrication of the thin film of the PI-2540 and PI-2610, dilution was required to achieve better rheological properties. It was suggested that when too dilute of a solution was used, problems might arise with the surface tension between the silicon wafer and PAA. Figures 25-27 show the film surface of BPDA-PPD, PMDA-ODA and BTDA-ODA/MPD films cured at 400°C for 30 minutes. The bubble on the film surface was obviously observed on the PMDA-ODA which has the higest viscosity percursor. A clear picture of the smoothness can be seen in the 3 dimensional picture. These images are inverted, such that peaks on the surface profile represent depressions on the surface, and the valleys in the image correspond to peaks on the surface. It was found that the lower viscous solution of PI-2579 gave the smoothest surface profile. Figures 28-30 show the surface of polyimide film coated on the Pt electrode which was fabricated on the fused SiO_2 wafer using a CVD process. The 25 times magnification image shows bubbles on the surface of the PMDA-ODA and less bubbles on the lowest viscous precursor BPDA/PPD and BTDA/ODA-MPD films.

To enhance the peel strength of the film on the silicon wafer, the adhesion promoter was used. Unfortunately, the surface profile was deteriorated, even though the peel strength was improved as seen in Figure 31. Figures 32- 34 show the high resolution images of the polyimide film surfaces

cured at 400 °C for 30 minutes on the Si<100> wafer at an area of 120 x 120 μ m taken by AFM. Similar to the images from the optical microscope, the AFM images are inverted. We can observe the roughness due to the bubble on the surface in the smaller surface area in those three images.

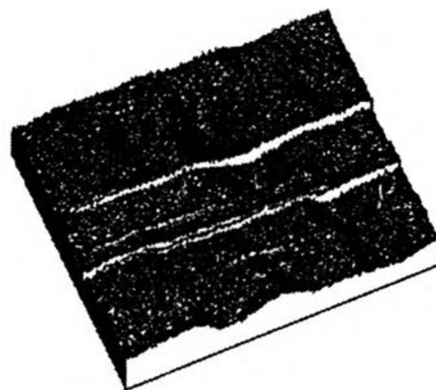

(25X magnification)

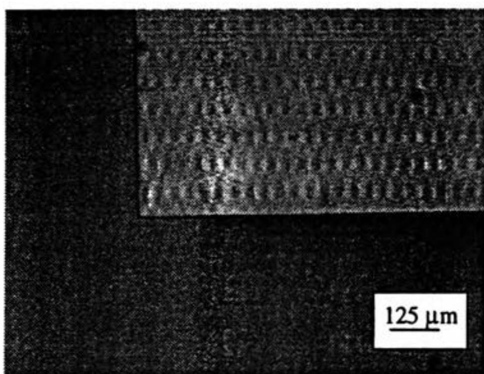

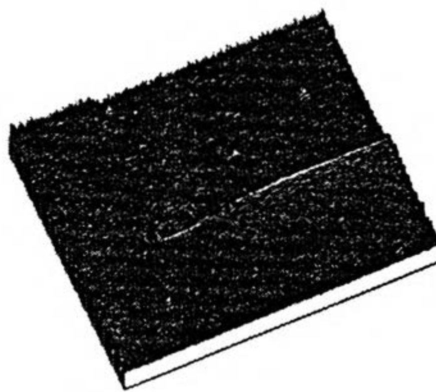

(200X magnification)

Figure 25 Optical Microscopic images of BPDA/PPD coated on Pt electrode on fused SiO_2 wafer cured at 400°C for 30 minutes.

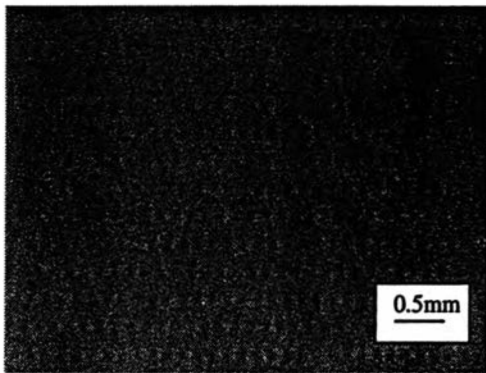

(25X magnification)

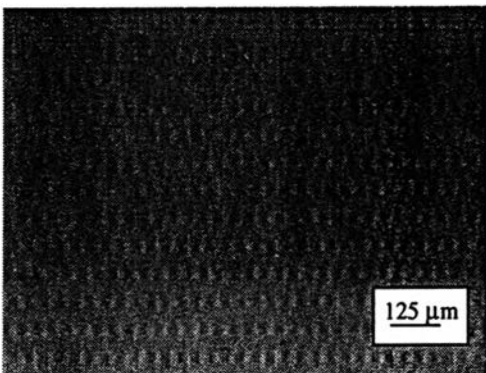

(200X magnification)

Figure 26 Optical Microscopic images of BPDA/PPD coated on Si<100> wafer cured at 400°C for 30 minutes.

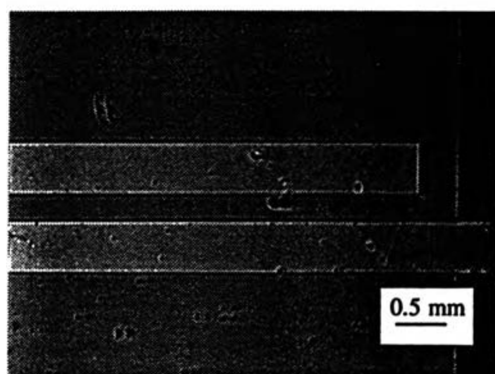

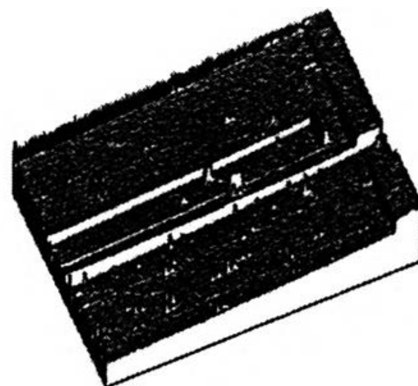

(25X magnification)

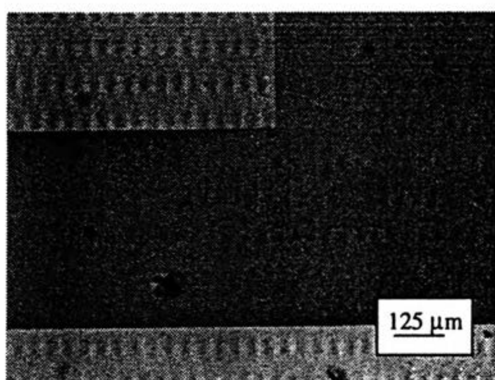

(200X magnification)

Figure 27 Optical Microscopic images of PMDA/ODA coated on Pt electrode on fused SiO_2 wafer cured at 400°C for 30 minutes.

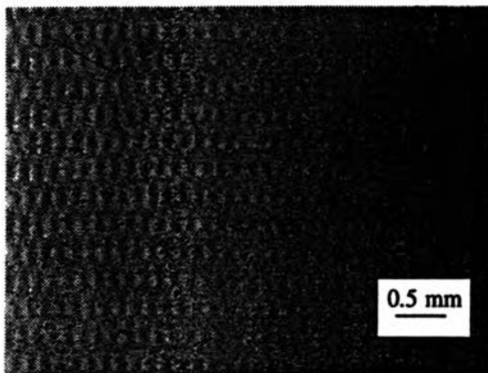

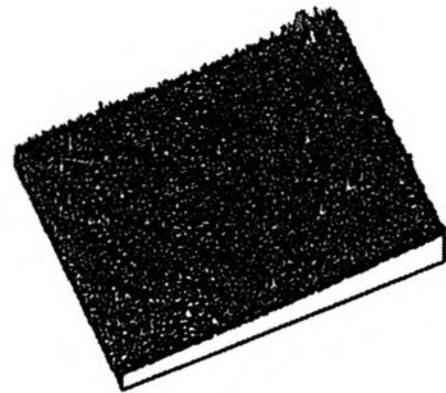

(25X magnification)

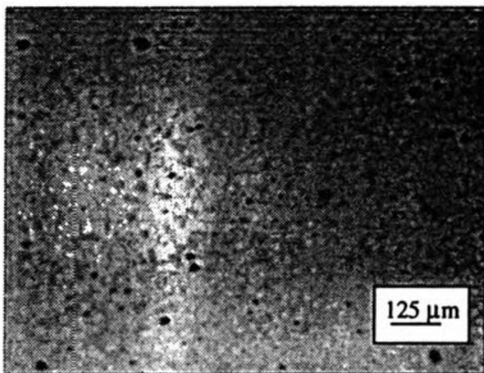

(200X magnification)

Figure 28 Optical Microscopic images of PMDA/ODA coated on Si<100> wafer cured at 400°C for 30 minutes.

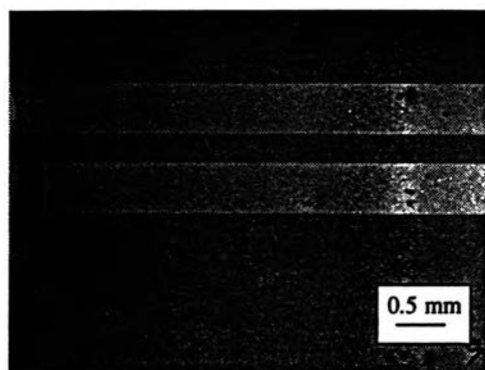

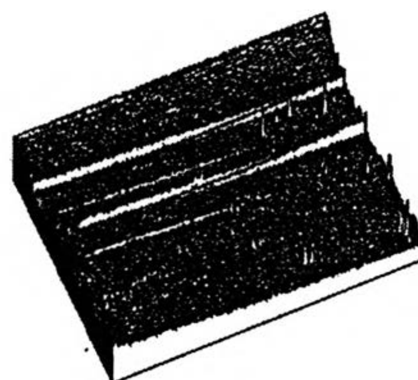

(25X magnification)

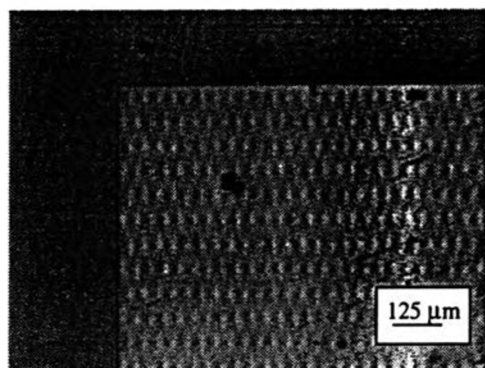

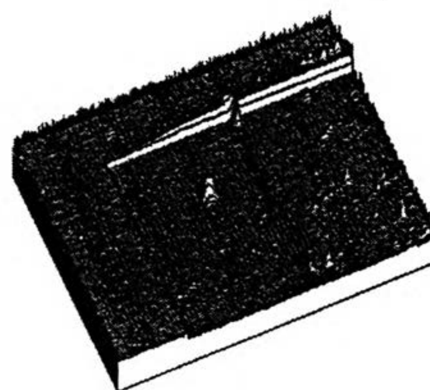

(200X magnification)

Figure 29 Optical Microscopic images of BTDA/ODA-MPD coated on Pt electrode on fused SiO_2 wafer cured at 400°C for 30 minutes.

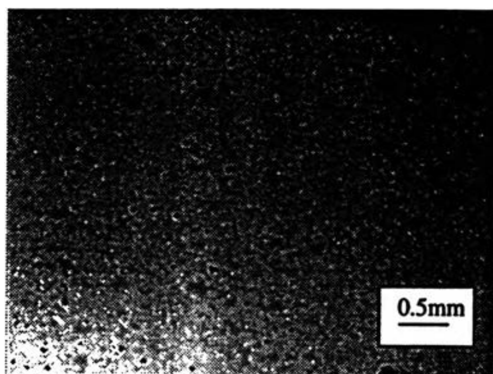

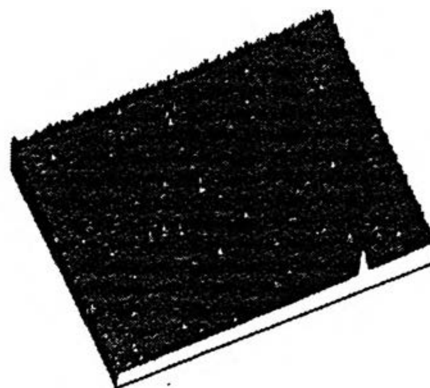

(25X magnification)

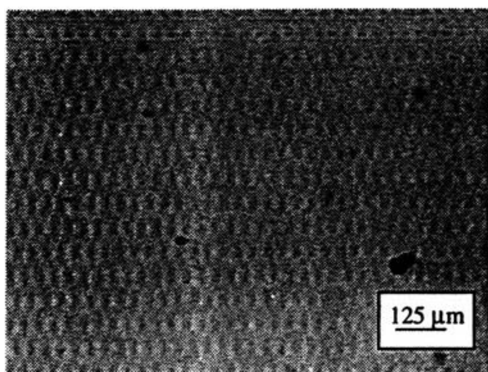

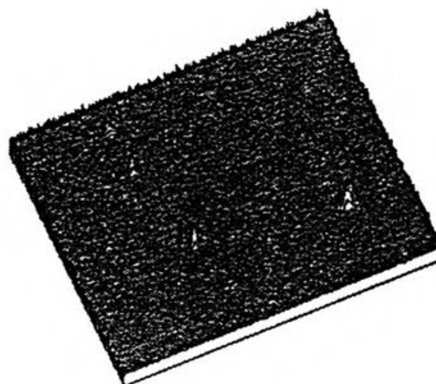

(200X magnification)

Figure 30 Optical Microscopic images of BTDA/ODA-MPD coated on Si<100> wafer cured at 400°C for 30 minutes.

(200X magnification)

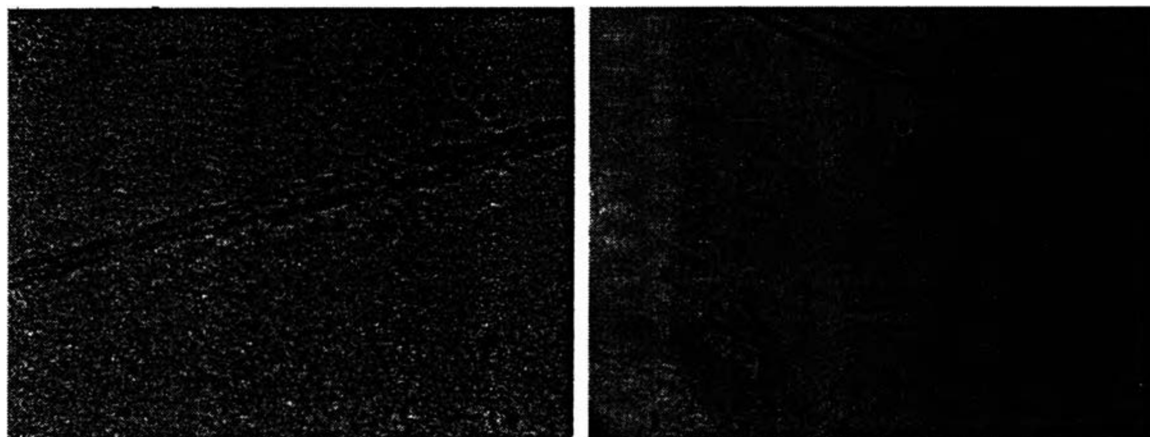

0.05 % adhesion promoter 0.1 % adhesion promoter

Figure 31 Surface images of BPDA/PPD coated on Si wafer with pre-applied 0.05 and 0.1% adhesion promoter on the surface.

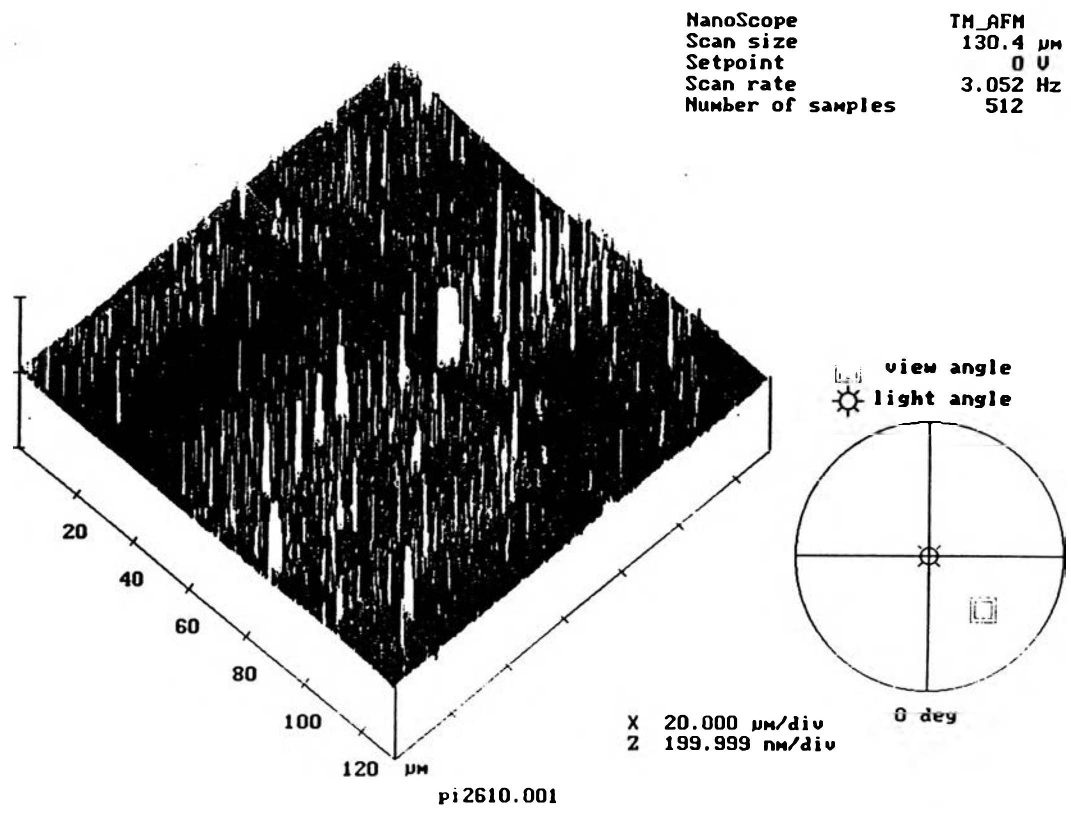

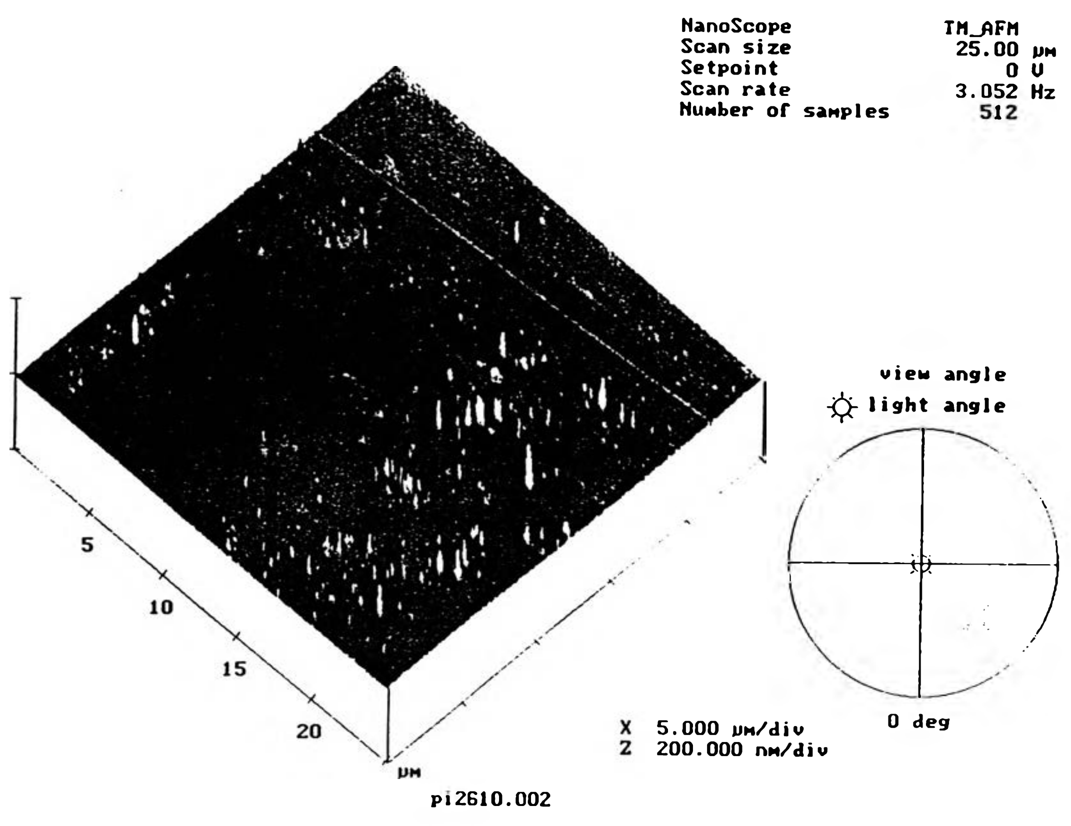

Figure 32 AFM images of the BPDA/PPD film surface cured at 400°C for 30 minutes on the Si<100> wafer.

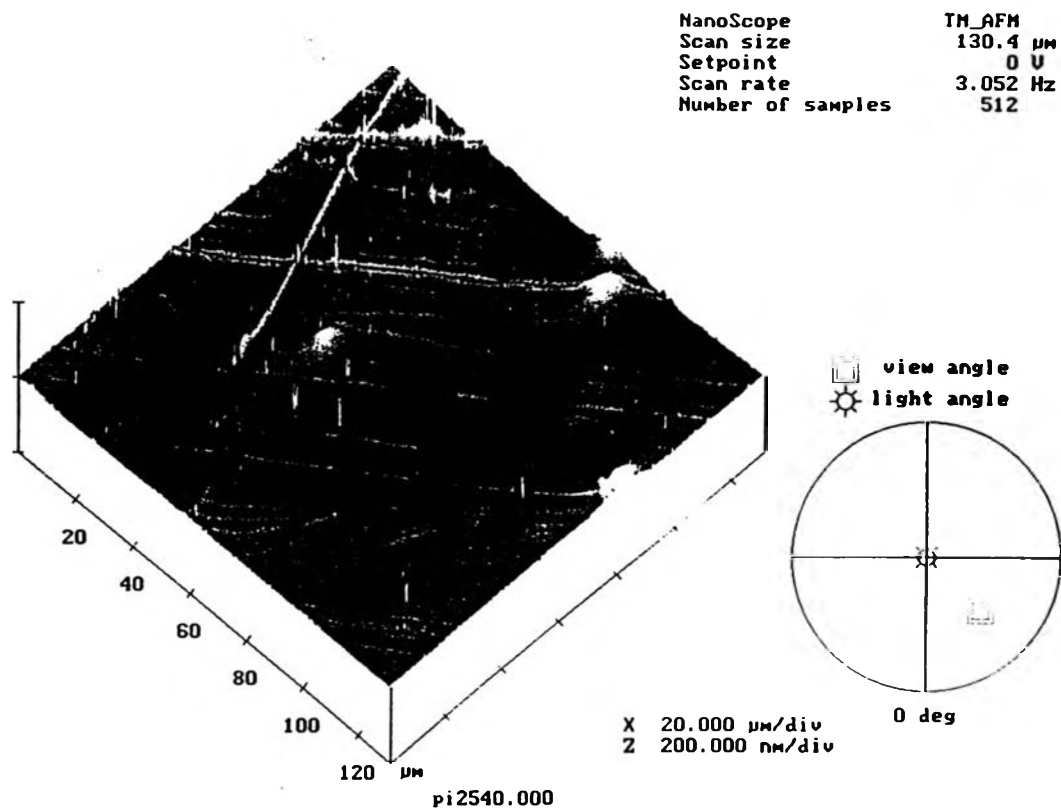

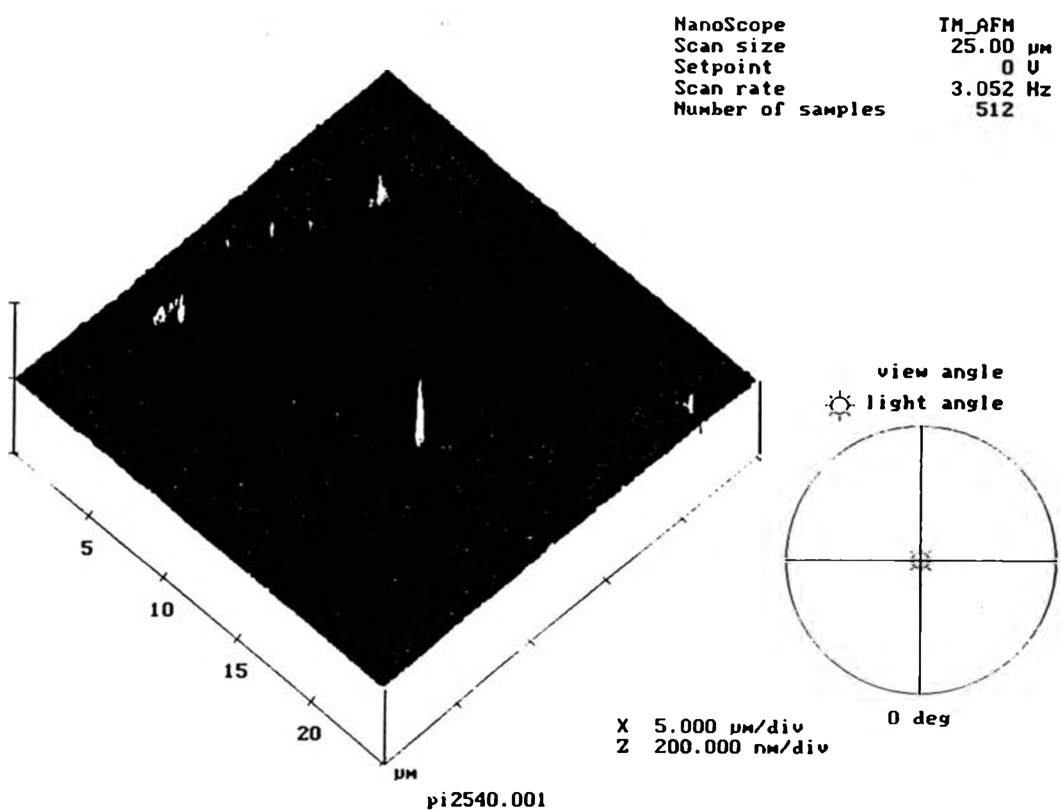

Figure 33 AFM images of the PMDA/ODA film surface cured at 400°C for 30 minutes on the Si<100> wafer.

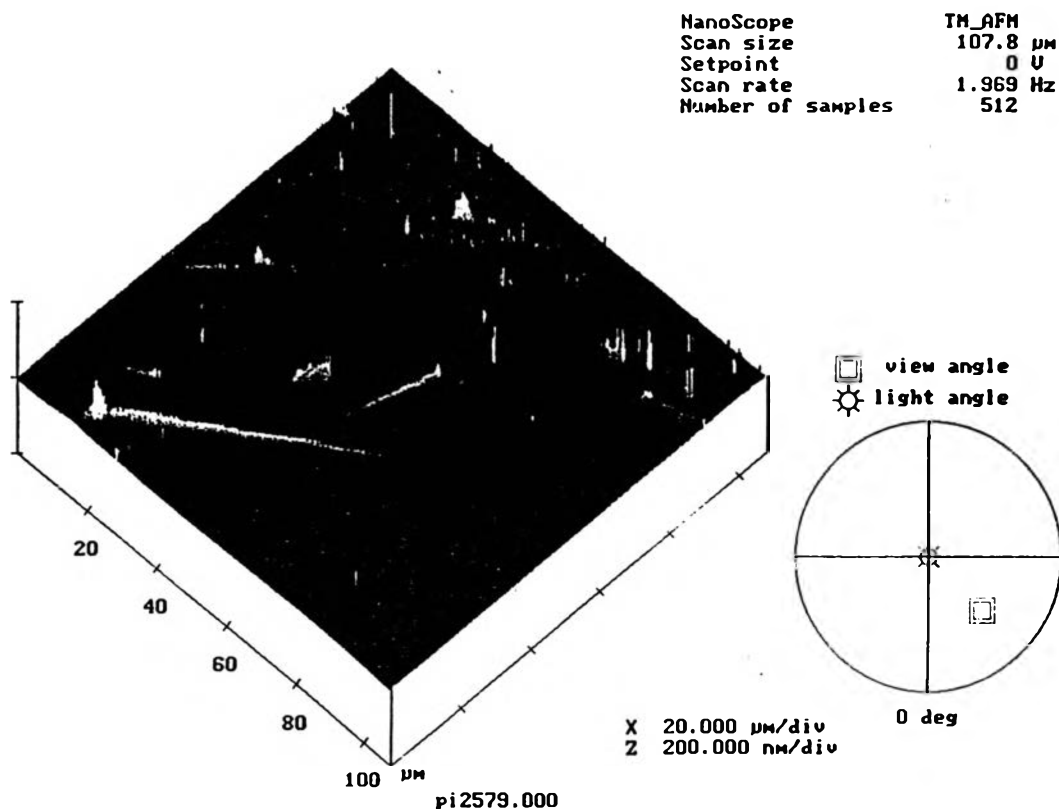

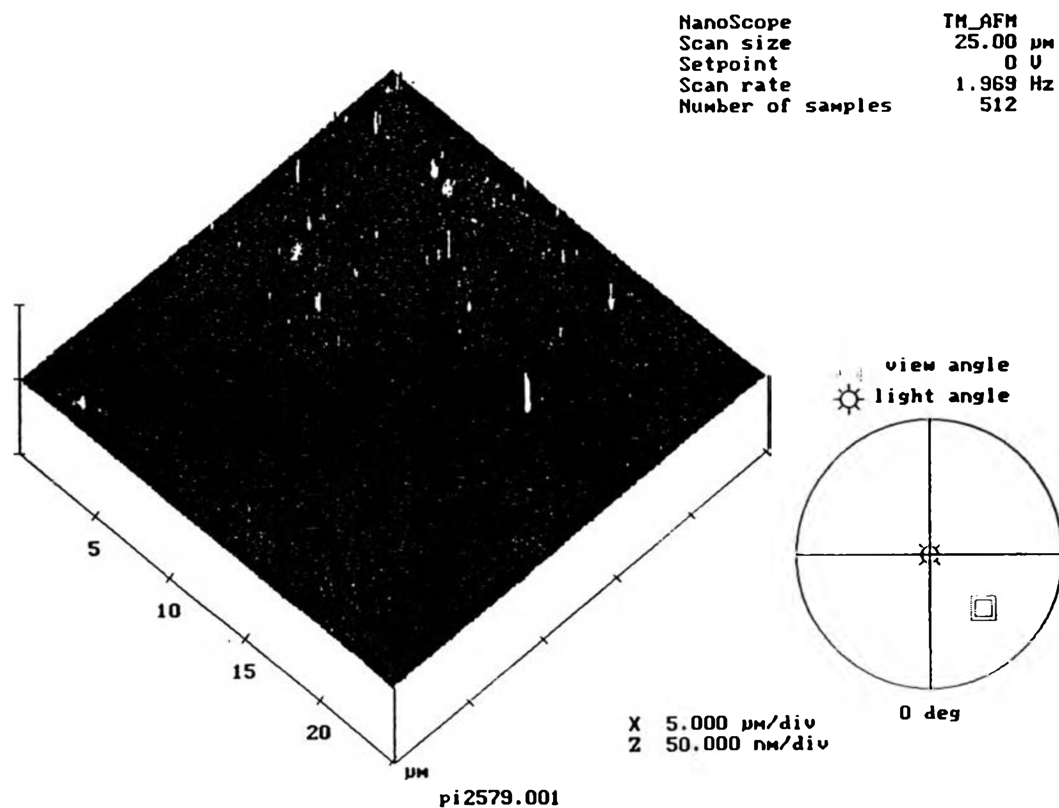

Figure 34 AFM images of the BTDA/ODA-MPD film surface cured at 400°C for 30 minutes on the Si<100> wafer.

3.6 Delectric Propeties

3.6.1 Dielectric Strength

The dielectric strength values for the three polyimide films and polyethylene are shown in Table 5:

Table 5 Dielectric strength of polyimide films compared with the insulating polyethylene film

Material	Thickness (mil)	Dielectric Strength (V/mil)			Standard deviation
		mean	max	min	
PI-2610 semirigid	0.64	6648	7703	5120	794
PI-2540 semiflexible	1.21	5396	6630	3708	787
PI-2579 flexible	0.71	5983	7543	4079	1112
Polyethylene	1.30	5259	6204	4865	394
Polyethylene *	1.00	4606	5330	4100	332

* Testing performed using a cylinder electrode, data came from ASTM Methods-D149.

The mean dielectric strength of the three polyimide films with ten measurements are higher than that of the polyethylene film at the same condition of experiment and with the cylinder electrode from the ASTM Method D-149. From Table 5, those values are belonging to the films with different thickness. As we knew that the thicker the films are, the higer the dielectric strength become. The most rigid film PI-2610 film, however shows the highest in dielectridc strength even it is the thinnest film.

3.6.2 Dielectric Constant and Dissipation Factor

Table 6 Dielectric constant and dissipation factor of polyimide films

	Polyimide Films		
	BPDA/PPD	**PMDA/ODA**	**BTDA/ODA-MPD**
Dielectric Constant at 1MHz	**1.45 ± 0.19**	**1.54 ± 0.21**	**2.54 ± 0.25**
Dissipation Factor	**0.31 ± 0.42**	**0.25 ± 0.04**	**0.46 ± 0.06**

The dielectric constant of the semirigid chain BPDA/PPD was lower than that of the semflexible PMDA/ODA and flexible BTDA/ODA-MPD. While the dissipation factor of those three films do not depend on the flexibility of the chain structure.